PROGRESS IN PHOTOVOLTAICS: RESEARCH AND APPLICATIONS
Prog. Photovolt: Res. Appl. 2010; **18**:511–515
Published online 15 July 2010 in Wiley Online Library (wileyonlinelibrary.com). DOI: 10.1002/pip.979

RESEARCH: SHORT COMMUNICATION

Fill factor analysis of solar cells' current–voltage curves

Johannes Greulich*, Markus Glatthaar and Stefan Rein

Fraunhofer Institute for Solar Energy Systems (ISE), Heidenhofstraße 2, D-79110 Freiburg, Germany

ABSTRACT

After completion of the solar cell manufacturing process the current–density versus voltage curves ($J(U)$ curves) are measured to determine the solar cell's efficiency and the mechanisms limiting the efficiency. An accurate and robust analysis of the measured curves is essential. In this work it is shown that fitting the two-diode model is inappropriate to quantify recombination in the space charge region and ohmic losses due to series resistance. Three fill factors, namely the fill factor of the illuminated $J(U)$ curve, the pseudo fill factor of the suns$V$oc curve and the ideal fill factor of the single diode model, are the base of a quick loss analysis that is evaluated in the present paper. It is shown that for an accurate analysis the distributed character of the series resistance and the network character of the solar cell cannot be neglected. An advanced current–voltage curve analysis including fill factors and fit is presented. Copyright © 2010 John Wiley & Sons, Ltd.

KEYWORDS

characterisation; electrical properties; fill factor; current voltage curve; network; fit

***Correspondence**

Johannes Greulich, Fraunhofer Institute for Solar Energy Systems (ISE), Heidenhofstraße 2, D-79110 Freiburg, Germany.
E-mail: Johannes.Greulich@fraunhofer.ise.de

Received 15 October 2009; Revised 2 February 2010

1. INTRODUCTION

At the end of the solar cell manufacturing process the current–density versus voltage curves ($J(U)$ curves) are measured to determine the solar cell's efficiency, the maximum power point and the mechanisms limiting the efficiency as there are resistive losses and recombination of electron hole pairs. An accurate and robust analysis of the measured curves is essential for the output power of the module and for the evaluation of the ongoing manufacturing process. The basic model for $J(U)$ curves, which is important for the following considerations, is the two-diode model. The current density $J(U)$ depends on the external voltage U in the following way.

$$J(U) = J_{\mathrm{Ph}} + J_{01} \cdot \left(\mathrm{e}^{\frac{U-J(U)\cdot R_{\mathrm{S}}}{V_{\mathrm{t}}}} - 1\right) + J_{02} \cdot \left(\mathrm{e}^{\frac{U-J(U)\cdot R_{\mathrm{S}}}{n_2 \cdot V_{\mathrm{t}}}} - 1\right) + \frac{U - J(U)\cdot R_{\mathrm{S}}}{R_{\mathrm{P}}} \quad (1)$$

V_{t} denotes the thermal voltage and J_{Ph} the photogenerated current density. The saturation current density J_{01} describes recombination of electron hole pairs in the base and in the emitter and J_{02} characterises recombination in the space charge region [1]. As usual the ideality factor of the second diode n_2 is set to $n_2 = 2$ throughout this work.

The two-diode model is a simple but useful model to describe the characteristics of crystalline silicon solar cells. In addition to the recombination losses (J_{01}, J_{02}) it includes the power losses due to series resistance (R_{S}) and parallel resistance (R_{P}). In this work R_{P} is assumed to be very large so that it does neither influence the cell's open circuit voltage nor its efficiency. Orthogonal distance regression based on weighted least-squares fitting [2] is one possibility to extract model parameters such as J_{01}, J_{02} and R_{S} from $J(U)$ curves. Fischer *et al.* [3] showed by simulations that the distributed character of the series resistance can cause severe deviations of the model parameters and misinterpretation of the measurements when fitting the two-diode model (Equation (1)) to measured $J(U)$ curves. In the present work we investigated different types of solar cells produced at Fraunhofer ISE using industrial processes. For every solar cell Equation (1) has been fitted to dark and illuminated $J(U)$ curves and to suns$V$oc curves using J_{Ph}, J_{01}, J_{02}, R_{S} and R_{P} as fit parameters. Comparing e.g. J_{02} from the illuminated fit with J_{02} from the dark fit, no good correlation is obtained. The same is valid for J_{01}. In general no consistent set of parameters can be found to describe all three curves with Equation (1), experimentally confirming Fischer's work. Besides, more interesting than the exact value of e.g. R_{S} or

J_{02} is how much efficiency η is lost due to R_S, J_{02} and other mechanisms.

A fill factor analysis can have these advantages. No fit is needed and fill factor and efficiency losses are directly obtained. By shifting the suns*V*oc curve along the current density axis by J_{SC} (1 sun) the pseudo illuminated curve and the virtually series resistance free pseudo fill factor pFF are obtained. The difference between FF and pFF then gives the fill factor losses due to the series resistance (R_S) [4]. The ideal fill factor FF_0 is free from losses due to series resistance and free from losses due to recombination in the space charge region (References [5] (p. 96) and [1] (p. 138)). It is calculated numerically from the ideal $J(U)$ curve:

$$J(U) = J_{Ph} + J_{01} \cdot \left(e^{\frac{U}{V_t}} - 1\right) \quad (2)$$

The two parameters J_{Ph} and J_{01} can be determined from two points of the illuminated $J(U)$ curve, e.g. under open circuit ($J(U = V_{OC}) = 0$) and under short circuit ($J(U = 0) = J_{SC}$) conditions since the influence of J_{02} on V_{OC} is small. The difference between FF_0 and pFF quantifies the FF-losses due to recombination in the space charge region (J_{02}).

2. EXPERIMENTAL

2.1. Increased pFF

In the research production line at Fraunhofer ISE the three fill factors are usually recorded for every cell for characterisation purposes. Surprisingly, increased pseudo fill factors with values close to and above the value of FF_0 are found at times for single and multi crystalline silicon solar cells. These cells exhibit slightly up to strongly higher series resistance and pFF–FF difference than usual. Such a cell is presented in Table I as an example. The specified J_{02} value is obtained from fitting the dark *IV* curve. This J_{02} value of the sample cell would cause $FF_0 - pFF \approx 1\%$ and thus contradict the small measured pFF–FF_0 difference. Many cells of this batch have a low finger resistivity of about 30 Ω/m and the emitter sheet resistance is about 65 Ω with standard front side metallisation on 2 Ωcm p-type Czochralski silicon. TLM measurements [6] revealed high contact resistance ($R_C > 10\,m\Omega cm^2$) for this batch.

After silver plating the contact resistance problem has vanished as expected [7], J_{SC} is reduced a bit due to broadening of the fingers and FF is on a standard level now. pFF is lowered compared to the measurement before plating, which can only partly be explained by J_{02}. From the two-diode model no influence of series resistance on pFF would be expected. Thus, this behaviour of the pFF cannot be explained by the two-diode model.

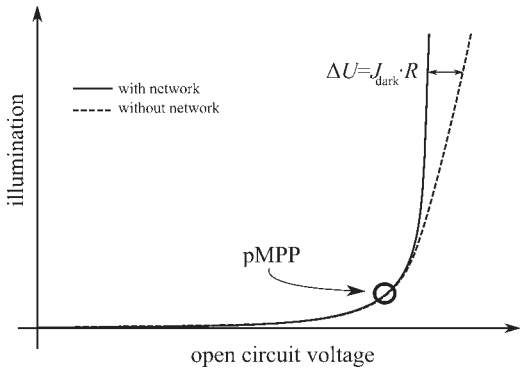

Figure 1. Sketch of two suns*V*oc curves with and without the influence of the network. Both curves have similar characteristics until pMPP is reached. The voltage drop ΔU caused by lateral currents increases with illumination and leads to an artificially increased pFF.

2.2. Network character of suns*V*oc

Looking closer at the suns*V*oc curves, it is easily seen that the distributed character of series resistance has to be accounted for [8,9]. V_{OC} is measured at the busbars that shade the underlying silicon completely when illuminating the solar cell from the front. In the shaded regions $J_{ph} = 0$ and thus the net current in these cell areas is the recombination current J_{dark}. This recombination current has to flow from the illuminated cell areas to the shaded areas through the emitter, the metal–semiconductor contact and through the metallisation finger. These three contributions to the series resistance are for a moment subsumed to the effective resistance R. The recombination current causes a voltage drop $\Delta U = J_{dark} \cdot R$ between illuminated and dark regions. With increase in illumination the voltage at the illuminated and dark diodes increases almost logarithmically. The recombination current of the dark diode rises exponentially with the voltage, causing a current through R and a voltage drop at R that are almost linearly increasing with illumination. This leads to a high pFF as can be seen in Figure 1.

Conversely, a smaller open circuit voltage leads to a smaller FF_0. Overall the FF_0–pFF is artificially reduced. pFF can be even higher than FF_0 in case of high recombination currents and high series resistances. This leads to misinterpretation of the fill factor differences since

Table I. *J*(*U*) data from a solar cell with increased pFF before (a) and after silver plating (b). The values of J_{02} (from fit to dark *IV* curve) are not suitable to explain the differences between pFF and FF_0. The R_S (calculated from comparison of illuminated and dark *IV* curve at MPP) is only slightly higher than usual.

	*V*oc (mV)	J_{SC} (mA/cm^2)	FF (%)	pFF (%)	FF_0 (%)	J_{01} (pA/cm^2)	J_{02} (nA/cm^2)
(a)	610.6	35.29	70.40	83.05	83.05	1.089	16.98
(b)	611.9	34.84	79.65	82.47	83.07	1.094	23.37

DOI: 10.1002/pip.979

the influence of series resistance and that of high recombination currents both influence pFF.

3. SIMULATIONS

3.1. Model

A simulation tool called FINEST (acronym for Fit and Network Simulation Tool) has been developed to further analyse the behaviour of the suns*V*oc curve. With this tool it is possible to quantify the effect described above, to see in which cases the network dominates and to check alternatives to get reliable measures for series resistance and J_{02}-like recombination losses. It simulates a quasi-2D network similar to the one described by Vishnoi *et al.* [10], accounting for different contributions to the series resistance and for shading by the front metallisation. Cell parameters as J_{Ph}, J_{01} and J_{02} can independently be set to different values in the three following cell regions: (1) the cell area covered by the metallisation fingers, (2) the area covered by the busbars and (3) the unmetallised cell area. Furthermore, the front grid design (finger and busbar width, number of fingers) can be varied. We use a 4th order Runge–Kutta–Nyström algorithm [11] to solve the differential equations for the unmetallised region

$$\frac{d^2U(x,y)}{dx^2} = R_{sheet} \cdot J(U(x,y)), \quad (1)$$

for the cell area under the grid fingers

$$R_{sheet} \cdot \left(J(U(x,y)) - \frac{U_f(y) - U(x,y)}{r_C} \right), \quad (2)$$

and for the grid finger itself

$$\frac{d^2U_f(y)}{dy^2} = R_f \cdot I_f(U_f(y)). \quad (3)$$

Here $J(U)$ is the current density as calculated by the two-diode model, $I_f(U_f)$ is the current density entering the finger from the emitter, U and U_f designate the voltage in the emitter layer and in the front metallisation finger, respectively, r_C is the contact resistivity and R_f the finger resistivity (see Figure 2).

The voltage $U = U(x,y)$ is locally applied to the two-diode model. Please note that the voltage is dependent on the position (x, y). As described above, the lateral variation

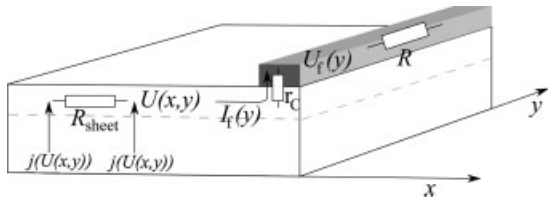

Figure 2. Sketch of a part of the solar cell. The potential of the emitter with sheet resistance R_{sheet} is $U(x, y)$, the potential of the finger (grey) with resistance R_f is $U_f(y)$.

Table II. Parameter boundaries for the network simulation with FINEST. The index 'nm' stands for the cell areas that are not covered by the front metallisation of the solar cell, the index 'met' for the metallised areas, 'av' stands for average value.

	minimum	maximum
r_c (mΩ·cm^2)	4	60
R_{SH} (Ω)	50	65
R_F (Ω/m)	20	100
J_{01}^{nm} (pA/cm^2)	0.6	1.0
J_{01}^{met} (pA/cm^2)	1.0	20.0
J_{02}^{hom} (nA/cm^2)	0	60

of $U(x,y)$ is caused by the series resistance and by lateral currents. If the lateral variation of $U(x,y)$ is large, then the lateral distribution of the saturation current densities is relevant. In this case the two-diode model with the averaged values of J_{01} and J_{02} is expected to deviate most from the quasi-2D model.

3.2. Approach

Using FINEST the influences of series resistance and lateral variation of the saturation current densities have been investigated. Namely the effect of emitter sheet resistance R_{sheet}, contact and finger resistivity and locally raised J_{01}- and J_{02}-like recombination on the pseudo fill factor have been studied. For the parameter values of the variation see Table II. Special focus has been put on those parameters that are not directly accessible by measurement and that are rather difficult to control in industrial solar cell production. These are the saturation current densities under the metallisation which can significantly deviate from the saturation currents under the unmetallised regions [12] and R_C and R_f. The pseudo fill factor pFF_{av} of the two-diode model with averaged saturation current densities has been calculated and compared to the pFF from the network calculations. The difference pFF–pFF_{av} is the increase of the pseudo fill factor due to lateral voltage deviations at the solar cell's surface. Least squares fitting of the two-diode model to each simulated illuminated, dark and suns*V*oc characteristics has been performed. A second fitting procedure limited to smaller current densities ($J < 3$mA/cm^2) has been done in addition for the dark and suns*V*oc curves to avoid a large influence of the lateral variation of $U(x,y)$ and to extract the averaged J_{01} and J_{02} as measures for recombination. The former fitting parameters are referred to as 'full range fit parameters', the latter as 'low J fit parameters'.

4. RESULTS AND DISCUSSION

4.1. Full range fit

Fitting the two-diode model (Equation (1)) to simulated illuminated, dark and suns*V*oc current voltage character-

istics over the full current range from $J=0$ to $J=J_{SC}(1\,\text{sun})$ cannot reliably reproduce the averaged saturation current densities. Due to the high currents and high lateral voltage variations the influence of the network character cannot be neglected. This explains to a large fraction the experimentally found contradictions within the fitted parameters that were mentioned in the introduction. They do not necessarily originate from using a wrong elementary model, which is the two-diode model.

4.2. Fill factor analysis

The data obtained from the network simulations are multivariate and cannot be analysed easily. Due to the high number of parameters that have been taken into account and their cross correlations it is not possible to deduce simple general rules to predict quantitatively how much the pFF is increased for a certain set of parameters. When restricting the analysed parameters to the fill factors and full range fit parameters, no general quantitative rules at all can be deduced. As an example Figure 3 shows the influence of finger and contact resistance on pFF–pFF_{av}. As can be seen, for a cell with standard parameters the pFF is increased by about 0.1%abs. to 0.2%abs.

4.3. Advanced analysis

As expected the low J fit parameters, particularly from the dark $J(U)$ curve, yield good correlation with the averaged saturation current densities that were used for simulation (see Figures 4 and 5). With these parameters it is possible to get rid of the network character and to calculate pFF_{av}. It

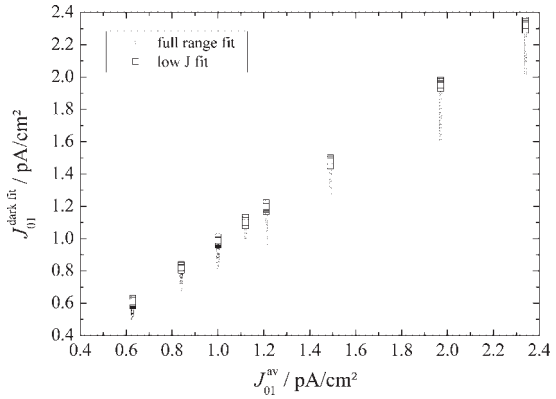

Figure 4. Averaged J_{01} versus fitted J_{01}. The full range fit does not reproduce the averaged values whereas the low J fit does.

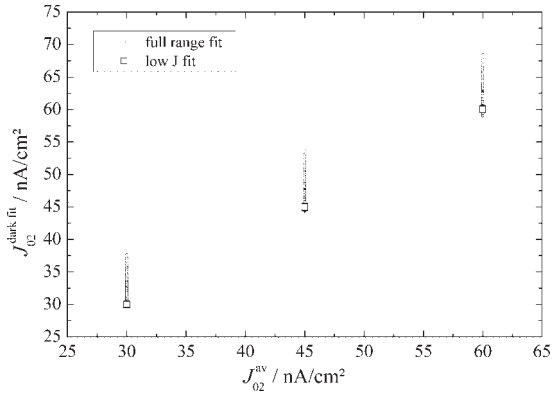

Figure 5. Averaged J_{02} versus fitted J_{02}. As for J_{01}, the low J fit yields the averaged J_{02} values.

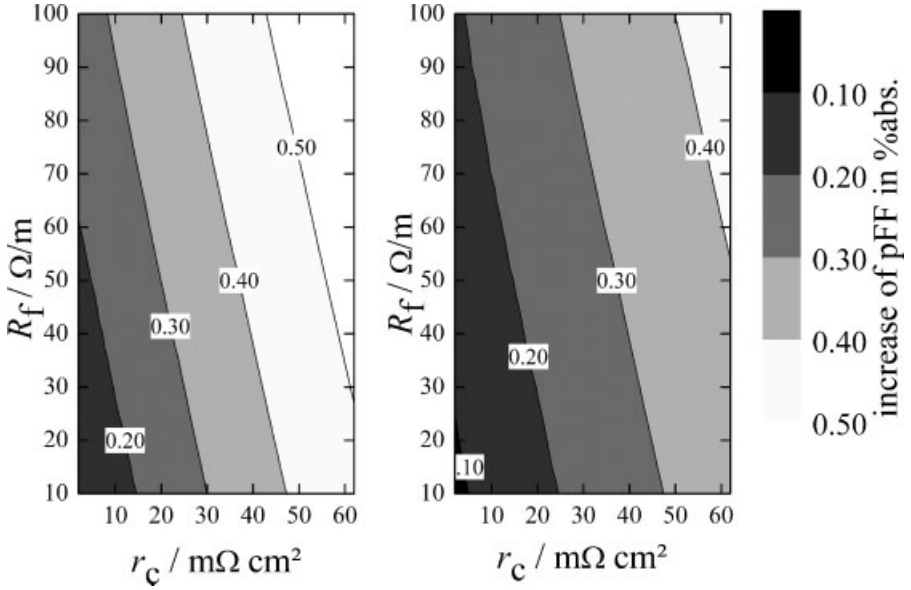

Figure 3. Increase of pFF due to the network character for varying finger and contact resistances. A standard solar cell has been simulated. J_{02} is completely concentrated under the metallisation (left) and homogeneously distributed over the whole cell surface (right).

is free from ohmic losses due to series resistance and series resistance induced network effects. The fitted J_{02} and FF_0–pFF_{av} are then reliable measures for recombination in the space charge region and/or any other non-ideal behaviour. As well pFF_{av}–FF is a reliable measure for series resistance related losses.

5. CONCLUSIONS

In case of high recombination under the front side metallisation of a solar cell and high series resistance, the fit of the two-diode model yields erroneous fit parameters. In such a case as well, the difference between fill factor FF and pseudo fill factor pFF and the difference between pFF and ideal fill factor FF_0 are misleading measures of series resistance losses and space charge region recombination losses, respectively.

The advanced method for characterising $J(U)$ curves that is presented here overcomes these difficulties. It includes fitting the two-diode model to those parts of the dark current voltage curve with small current densities. This yields the averaged saturation current densities J_{01} and J_{02} even if the network character dominates. Using these fit parameters and the two-diode model, reliable measures for fill factor losses due to series resistance and non-ideal J_{02}-like recombination can be obtained.

ACKNOWLEDGEMENTS

This work has been supported by internal project funding of the Fraunhofer Society and by the German Ministry for Environment, Nature Conservation and Nuclear Safety (BMU) within the framework of the project QUASSIM (0325132A).

REFERENCES

1. Würfel P. Physics of Solar Cells—From Principles to New Concepts. Wiley-Vch Verlag GmbH & Co KgaA: Weinheim, 2005.
2. Burgers AR, Eikelboom JA, Schonecker A, Sinke WC. Improved treatment of the strongly varying slope in fitting solar cell I-V curves. *Proceedings of the 25th IEEE Photovoltaic Specialists Conference*, Washington DC, USA, 1996; 1554, 1569–1572.
3. Fischer B, Fath P, Bucher E. Evaluation of solar cell J(V)-measurements with a distributed series resistance model. *Proceedings of the 16th European Photovoltaic Solar Energy Conference*, Glasgow, UK, 2000; 1365–1368.
4. Sinton RA. Possibilities for process-control monitoring of electronic material properties during solar-cell manufacture. *Proceedings of 9th Workshop on Crystalline Silicon Solar Cell Materials and Processes*, Golden, Colorado, USA, 1999; 67–73.
5. Green MA. Solar Cells: Operating Principles, Technology and System Applications. UNSW: Kensington, 1986.
6. Schroder DK, Meier DL. Solar cell contact resistance - a review. *IEEE Transactions on Electron Devices* 1984; **ED-31**: 637–647.
7. Pysch D, Mette A, Glunz SW. Comprehensive analysis of advanced solar cell contacts consisting of printed fine-line seed layers thickened by silver plating. *Progress in Photovoltaics: Research and Applications* 2009; **17**: 101–114.
8. Cuevas A, Lopez-Romero S. The combined effect of non-uniform illumination and series resistance on the open-circuit voltage of solar cells. *Solar Cells* 1984; Volume 11, Issue 2, Pages: 163–173 in the year 1984.
9. Harder N-P, Sproul AB, Brammer T, Aberle AG. Effects of sheet resistance and contact shading on the characterization of solar cells by open-circuit voltage measurements. *Journal of Applied Physics* 2003; **94**: 2473–2479.
10. Vishnoi A, Gopal R, Dwivedi R, Srivastava SK. Distributed parameter analysis of dark I-V characteristics of the solar cell: estimation of equivalent lumped series resistance and diode quality factor. *Journal of the IEE Proceedings Circuits, Devices & Systems* 1993; **140**: 155–164.
11. Nyström EJ. Über die numerische Integration von Differentialgleichungen. *Acta Societatis Scientiarum Fennicae.* 1925; **50**: 1–55.
12. Lenkeit B, Lauinger T, Aberle AG, Hezel R. Comparison of remote versus direct PECVD silicon nitride passivation of phosphorus-diffused emitters of silicon solar cells, *Proceedings of the 2nd World Conference on Photovoltaic Energy Conversion*, Vienna, Austria, 1998.